SAND2011-3711C

Proceedings of ASME 2011 5th International Conference on Energy Sustainability & 9th Fuel Cell Science, Engineering and Technology Conference
ESFuelCell2011
August 7-10, 2011, Washington, DC, USA

ESFuelCell2011-54453

AIMFAST: INITIAL DISH SYSTEM ALIGNMENTS RESULTS USING FRINGE REFLECTION METHODS

CHARLES E. ANDRAKA
JULIUS YELLOWHAIR
NOLAN FINCH
JEFF CARLSON
SANDIA NATIONAL LABORATORIES
ALBUQUERQUE NM USA

MATT FRANCIS
KIRBY HUNT
CARL RAFFA
STIRLING ENERGY SYSTEMS
SCOTTSDALE ARIZONA USA

TOM KULAGA
SOLUTION STREAM ENGINEERING
PHOENIX ARIZONA USA

ABSTRACT

The proper alignment of facets on a dish engine system is critical to the performance of the system. Improper alignment can lead to poor performance and shortened life, through excessively high flux on the receiver surfaces, imbalanced power on multicylinder engines, and intercept losses at the aperture.

Alignment approaches used in the past are time consuming field operations, typically taking 4-6 hours per dish with 40-80 facets on the dish. Production systems will need rapid, accurate alignment implemented in a fraction of an hour. In this paper, we present an AIMFAST characterization of a Stirling Energy Systems dish, before and after implementing an alignment using the AIMFAST software. The results of the alignment are correlated with fluxmapper measurements of the dish, and the improvement in the flux pattern projected to an engine receiver is calculated using Sandia's CIRCE 2 dish optical modeling tool. The alignment substantially reduced the peak fluxes on the flat fluxmapper targets as well as the projection onto the receiver. The fluxmap images correlate well with the CIRCE projections of measured facet normals. In addition, we implemented automated actuation of the facet during alignment, improving the response and accuracy of the system, resulting in total dish alignments with under 0.1 mrad RMS alignment error. We also implemented an adaptive alignment strategy that varied the alignment based on the AIMFAST-measured facet shape.

INTRODUCTION

Improper alignment of facets on a high-concentration dish system has been identified [1] as an important contributor to poor dish system performance. Most dish systems have had some sort of alignment adjustment capability, though a few dishes have been proposed or built with dimensional (fixture) alignment. Since very few dishes have been assembled in large quantities, alignment approaches have been limited to field implementations with manual facet actuation. This requires either climbing on structures or significant manlift operations. Diver et al [2] describes a number of common approaches used in the past. McDonnell Douglas [3] implemented a Digital Image Radiometer (DIR) alignment system consisting of a panel of computer-controlled light sources, with computer interpretation of the reflected images. These gave several points of data per facet, and automated the data collection and reduction process. However, data collection and reduction took several hours or more, and real-time adjustment was not accomplished. More recently, color lookback approaches [4, 5] have been successful in a laboratory field environment with high quality mirror facets. However, these alignment approaches are time consuming field operations, typically taking 4-6 hours per dish with 40-80 facets on the dish. Implementations of the color lookback method with production quality facets have been less successful, due to distortions of the reflected images. Production systems will need rapid, accurate alignment implemented in a fraction of an hour.

Alignment tools have usually consisted of a target mounted near the engine location, with a "distant" observer or light source [4], or at the 2-f location [5]. This often requires the dish to be placed in the horizontal (horizon) position, making access to the adjustments difficult and time consuming. In addition, the reflected light or image requires operator interpretation and a reasonably coherent image. Manufacturable facets may not have the image quality of laboratory dish systems explored in the past, making use of these alignment tools less effective. In a large field of dishes, a distant light or viewer may be blocked by other dishes.

The Sandia Optical Fringe Analysis Slope Technique (SOFAST) [6,7] was developed using fringe reflection techniques [8] to characterize facets and facet systems. Others [9,10] have also developed characterization systems based on fringe reflection techniques. Recent speed improvements in SOFAST for assembly line implementation have made it feasible to characterize the facet shape and rotations in near-real-time, making the use of this data feasible for alignment.

The fringe reflection technique, also called Deflectometry in some literature, is a dynamic target method of determining the surface normals at many points across an entire surface simultaneously. A camera is positioned so as to see the reflection of an active target in the specular surface of interest, Figure 1. A series of sinusoidal fringe patterns, or sinusoidally

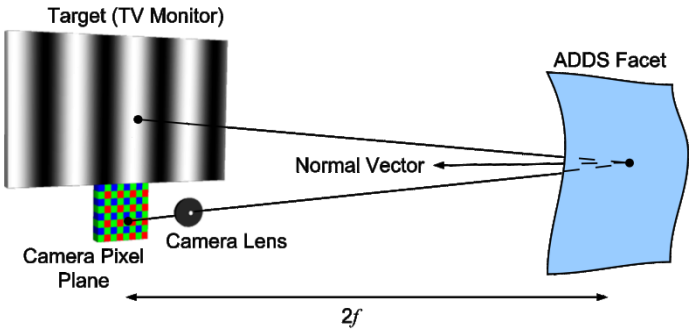

Figure 1.Fringe Reflection method physical layout

varying brightness patterns, are displayed on the monitor, and the reflected images are recorded. Initially, a single cosine wave is displayed, and then shifted 3 additional times by 90 degrees each shift. This process provides 4 brightness levels for each pixel of the camera. The phase angle of the pixel can then be determined as

$$\tan[\phi\ \ x,y)] = \left\lceil \frac{I_4 - I_2}{I_1 - I_3} \right\rceil \qquad (1)$$

Where I_n is the intensity measured at the camera pixel and n is the image sequence number. The phase angle is then simply the linear position on the screen. This process is repeated for horizontal and vertical directions. The results may be refined by displaying finer fringe patterns, using the initial single pattern for an absolute screen position. Given the camera lens position, the point at which each camera pixel ray intersects the specular surface, and the target point for each pixel, a field of surface normal vectors is developed. This set of normal vectors is integrated to a surface shape description. The process is iterated if the surface shape does not match design. The measured surface normals (slope) can be fitted to any representative surface shape equations if desired.

The fringe method does not rely on coherent images, so a 2-f approach with overlapping images on the target is feasible, leading to an alignment without extensive line-of-sight requirements, Figure 2. A LCD display is used as a target, collocated with a camera near the 2f location of the dish system. The solid black lines indicate the camera field of view, and the red lines indicate a typical camera pixel, reflected off the facets to the LCD screen. The system may be set up vertically, horizontally, or any convenient orientation. The colored panels, not used in the current implementation, will help automatically locate facets that do not hit the target area. The Alignment Implementation for Manufacturing using Fringe Analysis Slope technique (AIMFAST), based on SOFAST, has been implemented and tested at the prototype level [11]. This approach has been proposed to support production alignment of the Stirling Energy Systems (SES) SunCatcher™ dish-engine system. Table 1 provides a general description of the SunCatcher™ dish system used in this implementation of AIMFAST. In addition, a mobile version is proposed to perform re-alignment or assessment of deployed dish systems. The mobile system consists of a camera and monitor mounted on a pickup truck, supported with a laptop computer for data reduction, shown in figure 3. The concepts demonstrated with this system are directly applicable to the production facility implementation proposed. Further, in the latest testing, digital communication has been implemented from AIMFAST to automated actuators to accurately implement the alignment of a dish.

While [11] reported the first measurements with the AIMFAST system, this paper covers one of the earliest actual alignments of a dish system, with real-time tool feedback, and compares the measured results to fluxmapper images of the dish tracking the sun. In addition, the Finite Element Analysis, used to rotate the measurements to the tracking elevation position, has been refined to better represent the as-built dish structure.

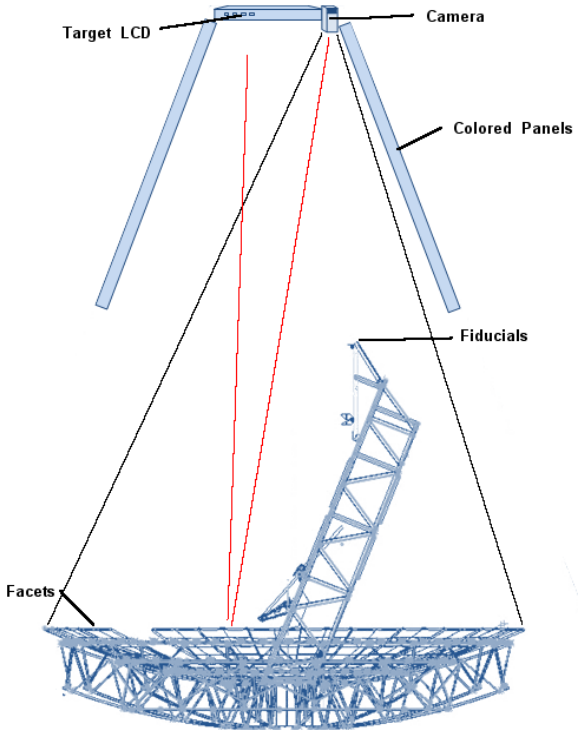

Figure 2. AIMFAST production physical layout with camera and target at the 2-f location.

Table 1. SunCatcher™ dish parameters

Parameter	Value
Layout	2-row radial gore parabolic dish
Facets	13 inner, 27 outer, 40 total
Diameter	11.4m
Intercept Area	89.5m²
Focal Length	6.705m
System Power	25kW$_e$ at 1000W/m²

Figure 3. TRUCKFAST implementation of AIMFAST, with a monitor and camera mounted in a pickup truck. The monitor is angled to align a dish in the below-horizon "service" position.

IMPLEMENTATION

The AIMFAST system currently consists of a NEC 70" LCD monitor, with a Basler 2.1 MPix camera mounted to the monitor parallel to the monitor surface normal. The use of a monitor rather than a projector system has the benefit of a known pixel spacing and lack of image distortion due to the projector lens and orientation. However, the target area is limited, so that this system may not be directly applicable to larger dish systems. On the current 11.4m diameter dish system, the target can "capture" facet pointing errors of about 10mrad in the horizontal and 25 mrad in the vertical direction. Facets that deviate beyond this range need to be manually positioned while viewing a camera preview image until the camera "sees" the target LCD in the facet. Generally speaking, capture could also be accomplished by manually leveling the edges of the facet with its neighbors. In production, automated "facet location" methods might include search algorithms, positional presets on the alignment tools, or colored cue runout areas surrounding the monitor to drive the facet toward the monitor location. The target must be large enough that a properly aligned dish reflects the camera lens to no more than 2/3 of the width of the target.

The camera is carefully aligned to the screen surface normal by projecting a spot with a laser square held against the screen, and centering the camera image on the laser dot 20-30 meters distant. The camera lens, a 6mm high quality c-mount lens, is characterized using the Cal Tech camera calibration toolbox for MatLab [12]. This removed barrel and tangential distortions from the images. The standard deviation of the residual pixel position error after calibration was about 0.55 pixel in each direction. While a simple model, modern accurate lenses are suitably characterized with this model.

The system is placed near the 2-f point of the dish, facing the dish. Alignment of the monitor and camera with the dish is a simple 3-step process. First, the approximate distance is checked with a laser distance finder, and the truck is moved until the distance matches design within 0.1 to 0.2m. Then the camera/monitor is tilted until dish is centered in the camera field of view. Finally, the dish is rotated until the view from the camera, reflected in the dish, is centered on the monitor. A system output that shows the camera reflected ray intersections on the screen is useful in this final step. Once the entire dish reflects the camera position to the screen, the "alignment" of the screen and camera is sufficient. The facets are pre-aligned during assembly with spacer blocks or other simple methods. In our case, the systems had previously been aligned with the color lookback method, providing a reasonable starting point, which facilitates getting the entire dish to reflect the screen to the camera. A fiducial reflector is placed on a stand mimicking the engine stand and located at the aperture center location, or two reflectors at the end of the boom. A pair of images is taken, one with the screen all black, the other all white, to form a mask image of the dish. From this image, a complex feature finding routine is used to locate the splits in the glass on each facet. These locations were determined to be more accurate and more repeatedly locatable than facet edges. These locations, along with the fiducial, are photogrametrically analyzed to extrinsically locate the camera, and therefore the screen, in 6 degrees of freedom relative to the dish. Three laser distance measurements are made to the dish to "true up" the distance along the dish optical axis, as this is the "weakest" degree of freedom in the single-image extrinsic analysis. The fiducial location is weighted equal to the number of points on the dish, so that the alignment is performed to the true boom line rather than perpendicular to the dish surface. This helps to account for imperfect boom alignment relative to the plane of the dish rim. Based on work under contract to Appalachian State University, we modified our feature finding routine to locate 3 points per facet, for 120 points total on the dish rather than the earlier implementation with only one point per facet. This was determined to improve the accuracy of the extrinsic location by a factor of 2, or under 1cm in x and y position. Any residual spatial positioning error of the camera/screen results in a slight alignment boresight error under 0.75 mrad, but does not affect the relative random alignment errors between facets.

The net result of the extrinsic analysis is the location of the camera, and thus the screen, in the dish global coordinate system. The dish coordinate system is defined from the vertex of the parabola, with x horizontal to the right when facing the dish, y upward, and z along the optical axis of the dish. Figure

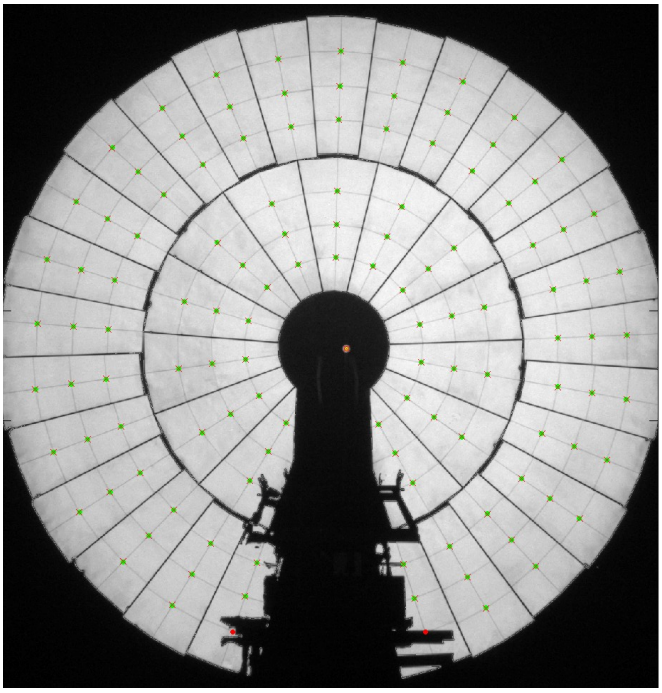

Figure 4. Differential mask image showing the located key points (green) and reprojected points (red "X") on each facet.

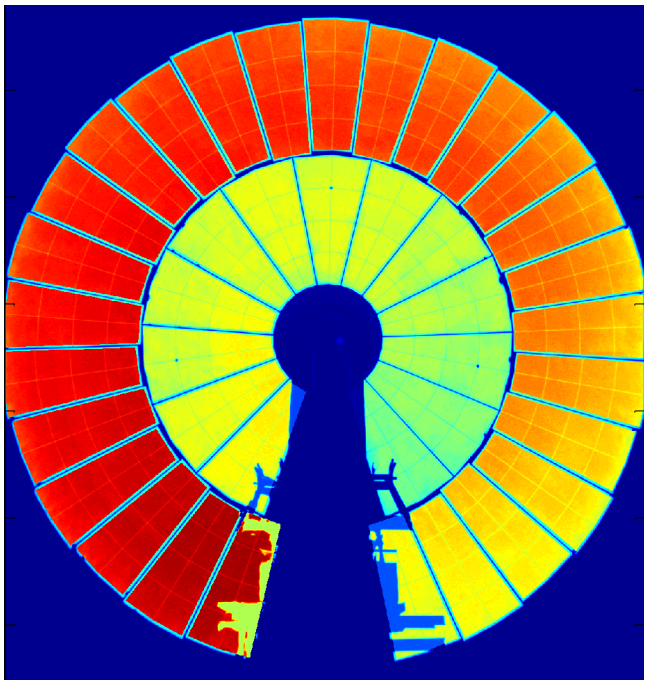

Figure 5. Facet masks used to identify pixels.

4 shows the differential image and the points located on the mirror surface. The green dots are the intersections of the lines, located through our feature detection algorithm. An X at each location indicates the reprojected points through the camera model form the extrinsic location, and red dots indicate points that were not successfully reprojected. The single yellow point in the middle of the dish is the reflective fiducial mounted at the engine aperture location. This appears slightly off center because the camera is not on axis, but is offset to the side of the screen. The midpoint between the camera and the center of the target screen is on axis. This offset is accounted for in the calculation of the normal vectors, and does not impact the accuracy of the normal vectors. The normal vectors are calculated from two vectors, formed by three points in space: The camera lens, the intersection of the camera pixel ray with the mirror, and the LCD target point determined by fringe analysis, with no requirement that any of these points be on a centerline.

From the mask image, we then parse out the "active", or reflective, pixels, assigning each one to a facet. This map allows selective characterization of each facet. We "erode" each facet pixel map by 4 pixels to remove any edge effects as the facets are rotated during alignment. Figure 5 shows the facet masks after corner location and pixel erosion. The facet masks are shown as a transparent overlay over the dish image, with an increasing color index per facet. Note that in the areas of boom clutter, the facet masks extend to the theoretical extents of the facet. Also note the 4-pixel erosion of the facet mask to eliminate edge effects.

During alignment, fringe patterns [6,7] are displayed, and the same technology used to characterize a facet in SOFAST is used to characterize these facets. We then compare each surface normal to the design surface normal at that point, determining a local slope error. Finally, we average these local slope errors across the selected facet to determine the tilt of the facet relative to design [13], and the required corrective rotation is reduced to mounting point linear adjustments.

The alignment strategy was developed for design facets using CIRCE2 [14] dish optical modeling tool. Once a design strategy provides acceptable flux distribution as modeled in CIRCE2, the strategy is directly provided to AIMFAST through reading the CIRCE2 input deck. In addition, we desire to align the dish perfectly at an intermediate tracking elevation, but we physically align the dish at or below horizon (or vertically in production). While AIMFAST could conceivably be implemented to align the dish at a tracking elevation angle by suspending the monitor and camera, a field implementation is more easily implemented at the service position where the monitor can be mounted in a truck. In production, the vertical alignment position provides worker access to the mirror adjustments without the use of personnel lifts, and important consideration for rapid alignment. Therefore, we rely on Finite Element Analysis of the dish structure to determine the rotations of the mirrors due to a varying gravity vector, and thus correct the alignment strategy based on predicted facet rotations. These FEA corrections are applied to the CIRCE2 ideal alignment strategy within AIMFAST, providing a skewed alignment at the selected alignment orientation. Figure 6 graphically shows the FEA-predicted facet rotations in moving form an intermediate tracking angle (40 degrees) to the service

position (-20 degrees). The rotations are primarily radial, resulting in a "blooming" motion of the facets with changing gravity vector. The maximum facet rotations due to gravity are about 1 mrad in magnitude. While the structure is quite stiff and the rotations small, a future paper will address a comparison between the FEA predictions and measured facet rotations with dish elevation. The magnitude of the facet rotations due to gravity, compared to goal alignment accuracies of 0.25 mrad, validate the need to correct for structural deflections form the alignment position to the "golden" elevation angle. Selecting a perfect alignment angle at an intermediate tracking elevation helps minimize the alignment error throughout the sun tracking elevation range. We do not, in the current configuration, attempt to resolve shape changes of the facets with elevation, instead assuming the facets are stiff. This is a reasonable assumption based on the design process for the facets.

In the latest AIMFAST implementation, we also generated optimized CIRCE2 decks for off-design facet focal lengths, which are occasionally encountered in the early production dishes. We demonstrated, through many CIRCE2 runs, that applying the optimized alignment strategy for each facet as measured in place gives an acceptable dish alignment despite differing facet focal lengths on a single dish.

Stirling Energy Systems (SES) developed an actuation tool to move the facets without human intervention or subjective input. The tool is capable of step movements of 25.4μm (0.001"). Two tools are installed manually to the outer

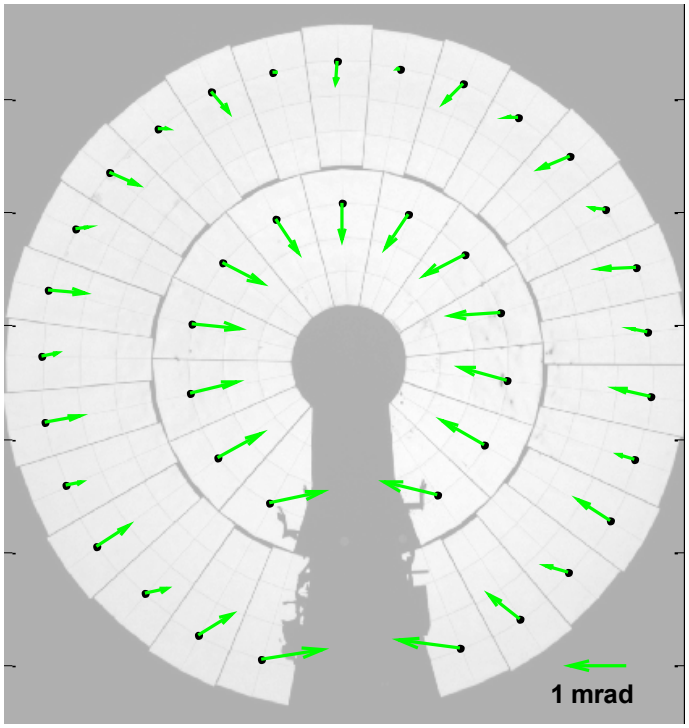

Figure 6. Facet rotations with elevation change predicted by Finite Element Analysis, in rotating the dish from 40 degrees elevation to the -20 degree alignment position.

tow mounts of the facet, and the adjustable mounts loosened. The operator then indicates the tool is installed by pressing a button. The SES tool communication software then requests AIMFAST to deliver data on that facet. The data delivered include the mount motions required, and a total magnitude of rotational error. When the indicated facet pointing error magnitude is below 0.1 mrad compared to the selected strategy for that facet, the software instructs the operator to lock the mount. Once locked, another reading is taken to confirm the results, and if acceptable, the operator is instructed to move the tools to the next facet. While highly automated, a software operator must monitor the stud adjustments to determine if a mount is stuck, which can happen due to corrosion, since the systems have been deployed for over a year. Later alignments were preceded by applying a penetrating oil to the mount before alignment, which greatly reduced instances of difficult mounts. Alignment time per dish was reduced to about two hours, with two operators in separate lifts applying and removing tools.

The actuation tools typically move 2-3 times to settle to an acceptable alignment. If the mounts stick, this may increase to ten or more iterations. Each iteration takes about 2.5 seconds to collect the fringe data, another 2 seconds to reduce the data, and about 2 seconds to actuate the tools. Therefore, the entire alignment step for each facet is typically less than 30 seconds. Multiple facets can be tested and reported simultaneously, since the camera images the entire dish at once. The communications program developed by SES manages the information flow, and can currently control up to 4 sets of tools, though only two were used in the present work. Figure 7 shows typical commanded motions on mirror adjustable mounts, demonstrating the rapid convergence of the method. While some facets were positioned within tolerance after 1 motion, 2-4 motions were typical. After the second move, the illustrated facet position was in specification, so no move was implemented, and the operator was signaled to tighten the mount. A final inspection verifies the facet did not move out of specification when the mount was tightened.

Initially, we aligned a single dish at Sandia, reported in

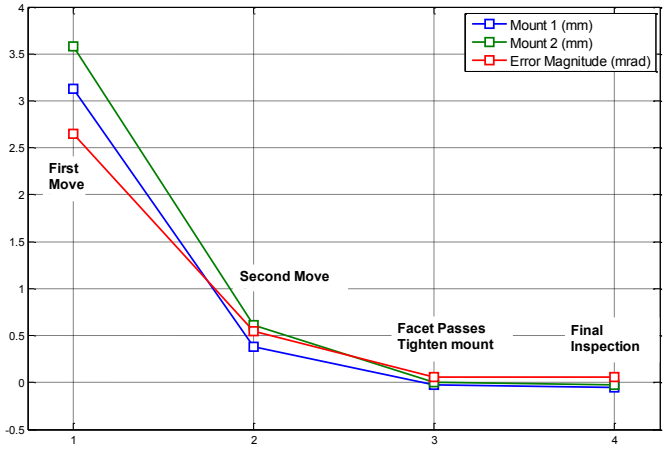

Figure 7. Typical commanded motions and confirmation measurements of a facet.

[11]. This implementation did not have communication to the tools, which slowed the operation. We then demonstrated the operation with tool communication at Sandia on a second dish, SES x0-4. This dish has some of the earliest pre-production facets, and the inner facet images overlapped and caused an unacceptable hot spot on the center cone of the receiver assembly. At this point, we proposed and developed the adaptive alignment strategy, which applied a different strategy to each facet based on the indicated facet focal length during the AIMFAST process. We then re-aligned dish x0-4 to within SES specifications for flux distribution.

Based on our success at Sandia, we transferred the technology to SES Maricopa, as part of the post-production upgrades scheduled at the plant. A series of product improvements are being tested on a subset of the dishes, including the improved alignment tools and techniques. We initially demonstrated the alignment on a single dish, number 111, at Maricopa. This system will be used as an example in this paper. After success on this dish, AIMFAST was applied to a product improvement subset of 12 dishes, using SES-supplied labor and engineering. The ease of use and accuracy of the system was clearly indicated in the rapid alignment process and the rapid learning curve. Each dish was confirmed after alignment using fluxmapping images in the vicinity of the engine heater head, as well as CIRCE2 projections of the flux onto the receiver cavity.

Dish 111 was initially selected because some experimental work had been performed with "hot alignments", or adjusting the mirrors while observing an image with the dish on sun. This had left a rather poor alignment, which resulted in high peak fluxes on the tubes, and a high "quadrant delta". The quadrant delta is the difference in gas temperature from the hottest cylinder to the coldest on the four-cylinder engine. A high quadrant delta results in reduced performance, as the system controls engine pressure based on the hottest cylinder. The colder cylinders operate at lower efficiency due to Carnot effects.

RESULTS

The AIMFAST data for the entire dish consists of 3-D coordinates of each camera pixel location on the facets (the point at which the camera pixel ray intersects the facet surface), a surface normal at that location, and the area covered by that pixel. This data can be entered into a ray trace or other optical analysis to determine the flux pattern on an arbitrary receiver shape. A dish reflected energy image analytically projected onto a flat target can be qualitatively or semi-quantitatively compared with fluxmapper results to confirm the alignment. Then the CIRCE2 (ray trace) analysis model can project the image onto the actual receiver geometry to determine the incident radiation on various receiver surfaces. Each facet definition contained roughly 20,000 data points, each about 1cm square.

Figure 8 shows the CIRCE2 prediction using measured AIMFAST data prior to alignment, on a flat plate 6.909m (272") from the dish vertex, or 0.2m (8") behind the design focal plane of the dish. The AIMFAST data is collected at -20 degrees elevation, and corrected by the FEA data to the +40 degree tracking elevation, for comparison with sun-tracking fluxmap images. The fluxmap in this case was performed at 36.5 degrees elevation. The circular target is 0.61m (24") in diameter to match the fluxmapper target in the other images. The colorbar used in all of the images ranges from 0 to 110 W/cm². Figure 9 shows the measured flux pattern at the same location using the fluxmapper. The correlation between this fluxmap and the CIRCE2 prediction is quite good qualitatively.

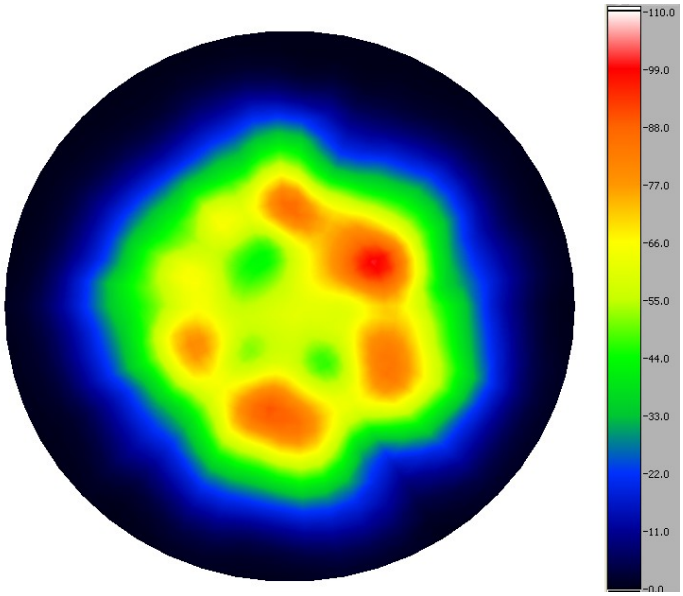

Figure 8. CIRCE2 prediction of flux on a flat plate in the vicinity of the heater head tubes, using AIMFAST-generated surface normals on the dish facets. The target is 0.61m (24") in diameter, and placed 0.2m (8") behind the dish focal plane. The flux colorbar ranges from 0 to 110 W/cm². The same scaling is used in all images.

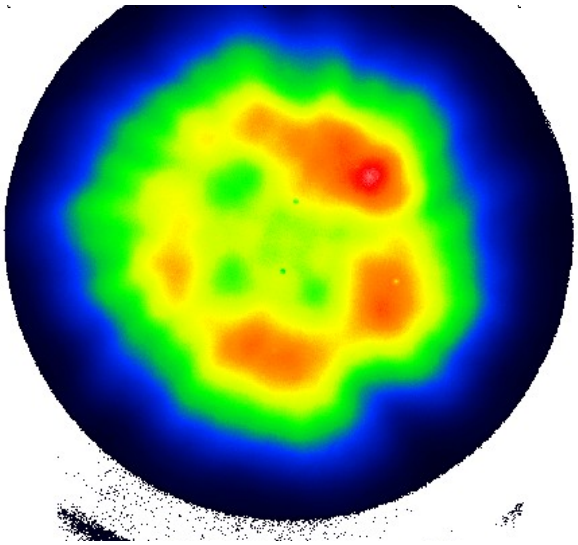

Figure 9. Fluxmap image of dish 111 on a flat target at the same location as the CIRCE2 analysis of figure 5.

The fluxmap appears to pick up more detail at the outer edges of the primary flux area. This is likely caused by the limited discretization in CIRCE2, with 50 circumferential nodes (7.2 degree node spacing).

As seen in the prior extrinsic analysis (figure 4), there is some blockage by the boom from the camera at the 2f location. We determined the measured facet shape, fitted with a Zernike-like monomial [6],

$$z=Ax^2+By^2+Cx+Dy+Exy+F \qquad (2)$$

where x and y are in the individual facet coordinate systems, with x aligned with the radial centerline of the facet, z is the optical axis of the facet, and y is perpendicular to both. This monomial fit was used to "fill in" this missing data, as the boom does not block the sunlight (infinite source position) in these areas. However, only the raw surface normal vectors are used to determine and correct the alignment error.

Figure 10 shows the CIRCE2 projection of this data onto the receiver surface and center ceramic cone. The receiver diameter is 0.357m (14"), with a center ceramic cone 0.129m (5") diameter. The model includes a 0.228m (9") diameter aperture ring. The model indicates incident concentrated solar radiation, but is not resolved to a "net" radiative flux on the surface, which would require a multimode cavity model. The peak flux on the tubes is about 110W/cm², well above SES's prescribed limits. The model indicates a 99.7% intercept factor with this aperture, so the initial alignment does not greatly degrade the intercept. The misalignment of the dish is shown in figure 11. The blue vectors indicate the resultant alignment error, anchored graphically to the inner mount/pivot, and the red vectors indicate the adjustments needed at each outer mounting location. An upward red vector indicates a longer mount is needed, downward means shorter. The error pattern

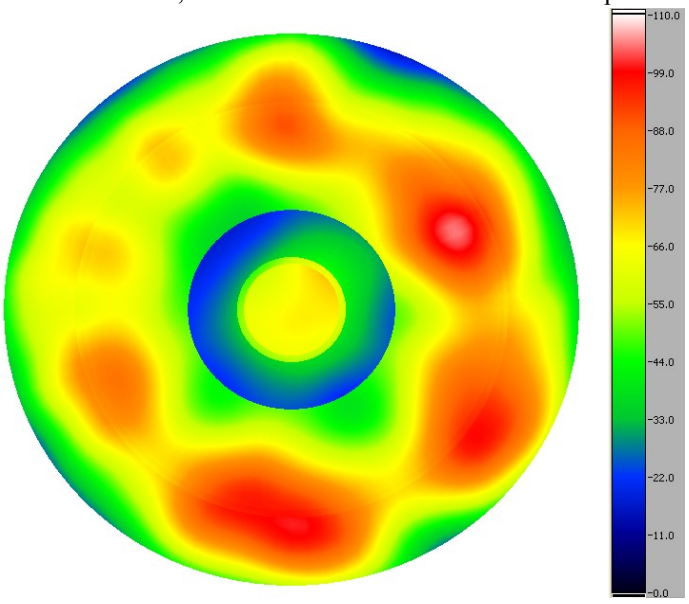

Figure 10. CIRCE2 projection of flux pattern onto the receiver absorber and center cone.

indicates a mix of systematic and random error in the prior alignment. The blue error vectors indicate a mix of radial and circumferential adjustments are needed. All adjustments are made to the outer two mounts, where radial adjustments are effected by simultaneous adjustment in the same direction, and circumferential by simultaneous adjustment in opposite direction.

After alignment, AIMFAST indicates a random alignment error (standard deviation) of 0.11 mrad in each axis (x and y of dish global coordinates), a mean error of -0.02 mrad in x and 0.12 mrad in y, and a total RMS (Root, Mean, Square) alignment error of 0.14 mrad in each axis. The mean error can be considered a "boresight" error, in which the alignment is slightly off center at the engine. Our goal had been 0.25 mrad RMS in each axis, as recommended in [1]. The post-alignment error plot is shown in figure 12. Continued application and refinement of processes led to consistent results at less than 0.1 mrad RMS on later dishes. Note that the residual alignment errors are as reported by the AIMFAST tool. A future paper will cover a complete sensitivity and error analysis of the AIMFAST tool. At this point, these should be considered "relative" accuracies, and compared to the pre-alignment status.

A CIRCE analysis on a flat target, figure 13, FEA-corrected from the -20 degree measurement to a 30-degree tracking angle, shows a good correlation to the fluxmap at 29.5 degrees elevation, figure 14. Once again, the flux profile is presented on a 0.61m (24") diameter flat plate 6.909m (272") from the dish vertex, or 0.2m (8") behind the design focal plane

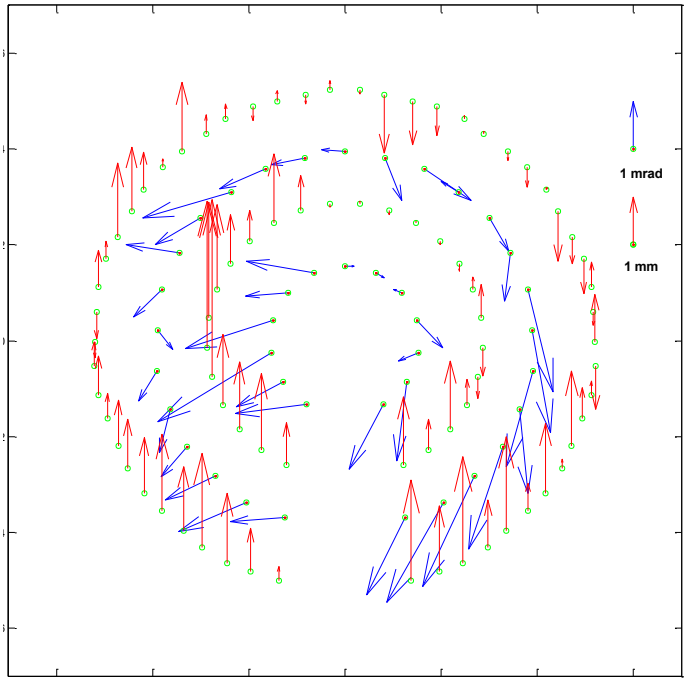

Figure 11. Mirror tilt errors as determined by AIMFAST. The blue vectors represent the magnitude and direction of the mirror tilt away from the alignment strategy. The red vectors indicate the magnitude of the outer mirror mount adjustments needed to resolve the error.

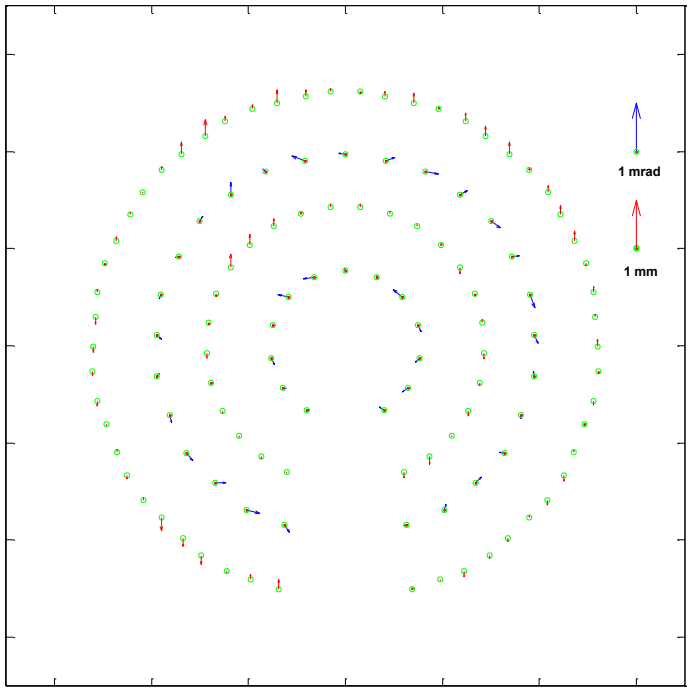

Figure 12. Error plot of dish 111 after AIMFAST alignment.

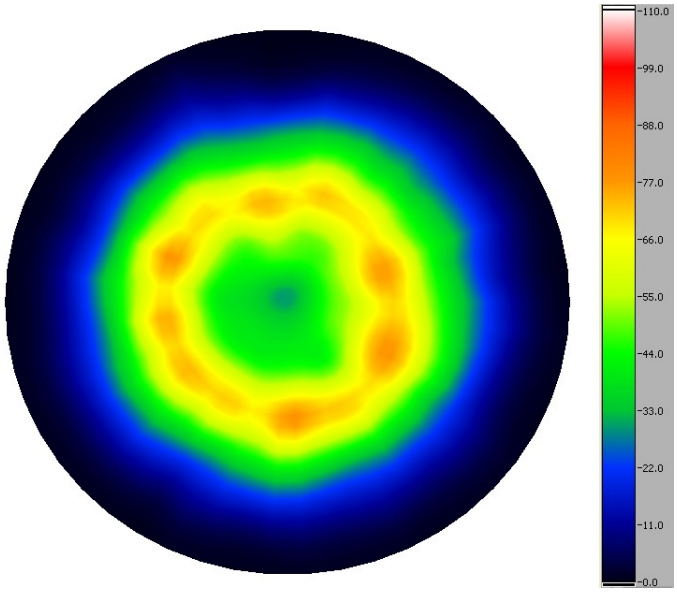

Figure 13. Post alignment CIRCE2 prediction of flux on a flat target near the receiver absorber tubes. The scale is set to the same range as figures 5 and 7.

of the dish. The flux scaling matches the prior images, with a range of 0 to 110W/cm² on the colorbar. Again, higher detail levels are seen in the fluxmap, probably due to the limited resolution of the CIRCE evaluation. The peak flux on the flat target as determined by CIRCE2 is about 78 W/cm². The qualitative and semi-quantitative match between CIRCE2/ AIMFAST results and the fluxmapper supports the assertion

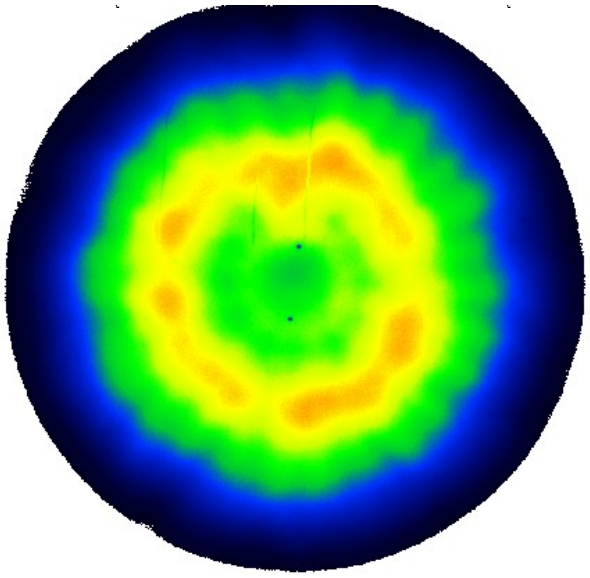

Figure 14. Fluxmap image of dish 111 after AIMFAST alignment.

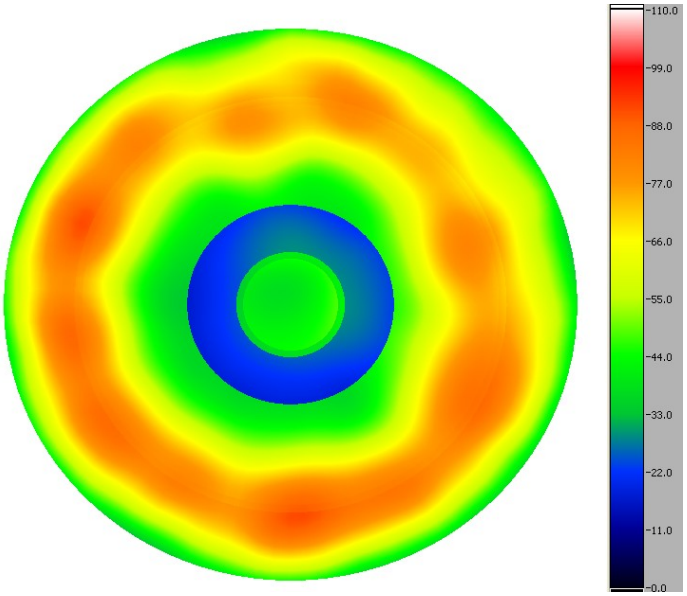

Figure 15. CIRCE2 predicted flux on the receiver assembly after AIMFAST alignment, showing a dramatic reduction in peak flux. The scaling is consistent with figures 5 and 7.

that the alignment is substantially improved, and that the FEA analysis is reasonable.

The data was then projected to the receiver, figure 15. The peak flux on the tubes was reduced to below 90 W/cm², which is within specification. The remaining "ring" of higher flux is caused by most of the inner facets, an early production model, being shorter than design in the radial focal length [1]. The alignment strategy was designed to reduce peaks on the center plug, which was successful, with a peak under 50 W/cm², at the

expense of higher but acceptable peaks on the absorber tubes. The aperture intercept did not change, and was again 99.7%. This is an important distinction between high performance (high flux) dish systems and troughs. While the alignment was substantially improved in terms of peak fluxes and quadrant balance, the intercept factor was unchanged. Therefore, characterization of dish alignment strictly through intercept factor has limited value.

The system was then operated with the same engine on sun. The quadrant delta was reduced from about 100°C to 14°C, a remarkable reduction. This results in an additional 0.25 to 0.5 kW of net output power (1-2%) under similar operating conditions. In addition, the reduction of peak flux on the absorber tubes to within specification is expected to have a dramatic impact on tube life.

SES has continued to apply AIMFAST to 1-2 dishes per night. The alignment process has become routine, with temporary technician help for operators. The alignment process is typically completed in 2 hours, and the results obtained are similar to dish 111. The fluxmap images match the CIRCE predictions with measured data quite well.

CONCLUSIONS

A method for rapid evaluation and alignment of dish systems, AIMFAST, has been demonstrated. The close correlation of the measured data as projected by CIRCE2 and the fluxmap measurements on the dish give high confidence that the process can be used for accurate alignment. We achieved alignments with tool-indicated total errors of less than 0.1 mrad RMS in each dish axis, well within the needs of this dish system. The fluxmap comparisons include FEA structural rotation corrections to the measured alignment data. The structural rotations determined by FEA are large compared to the alignment residuals, so the correlation of results verifies that the FEA model is reasonable. At a system level, the improvement in system performance, evidenced by quadrant delta and output power, was dramatic. The closed-loop automated tooling makes the implementation of the alignment simple, accurate, and in near-real-time, demonstrated through a limited skill temporary field workforce..

The AIMFAST system, demonstrated in a truck-mounted field-retrofit condition, is suitable for mass production and assembly in an assembly plant on site. SES has a goal of just over 20 minutes for alignment. This system is easily capable of such, depending on how many tool sets are simultaneously installed on the dish.

The techniques used in AIMFAST are currently hardwired to some dish features of the SES system. However, our next step is to generalize the processes, particularly for facet description, key point location, and actuation, to support most dish configurations. We also intend to extend this technology to heliostats. The techniques can also be applied to dish characterization without alignment, as facets that are discontinuous are considered separately in the analysis. While the alignment process was considerably faster than other methods, and fully removed subjective evaluation, production will require faster processes. It is clear during this process that the majority of time is spent moving the lift to the next facet. In production, this indicates a need to align in a facility with full access to the adjustments, rather than in the field with lifts. With such an arrangement, a 20-minute alignment of a 40-facet structure is entirely feasible.

While the AIMFAST tool indicated substantial alignment accuracy, backed by fluxmap images, it will be important to complete a full error analysis in a future paper. In addition, this method relies on accurate Finite Element Analysis of the dish structure. While modern FEA tools are reliable, it is important to test the accuracy. We plan to use the AIMFAST tool to measure the facet rotations at various elevations, and compare the rotations to the FEA predictions, again in a future paper. Further, facet shape changes with elevation should be evaluated, and could be added to the tool.

ACKNOWLEDGEMENTS

This manuscript has been authored by Sandia Corporation under Contract No. DE-AC04-94AL85000 with the U.S. Department of Energy. The United States Government retains and the publisher, by accepting the article for publication, acknowledges that the United States Government retains a non-exclusive, paid-up, irrevocable, world-wide license to publish or reproduce the published form of this manuscript, or allow others to do so, for United States Government purposes.

The authors would like to thank Stirling Energy Systems for access to their systems during the development of AIMFAST, and access to data to demonstrate the quality of alignment. The cooperation with SES has made significant advances in dish-Engine technology possible.

References

[1] Andraka, C.E., Yellowhair, J, Iverson, B.D., (2009). “A Parametric Study Of The Impact Of Various Error Contributions On The Flux Distribution Of A Solar Dish Concentrator”, *Proceedings of the ASME 2010 4th International Conference on Energy Sustainability*, Paper ES2010-90242, ASME, Phoenix AZ USA May 17-22

[2] Diver R.B. (1992), "Mirror Alignment Techniques for Point-Focus Solar Concentrators." , SAND92-0668, Sandia National Laboratories, Albuquerque NM USA.

[3] Blackmon J.B., Stone K.W. (1993), “Application of the Digital Image Radiometer to Optical Measurement and Alignment of Space and Terrestrial Solar Power Systems”, *Proceedings of the 28th Intersociety Energy Conversion Engineering Conference,* Atlanta, Georgia, USA, August.

[4] Andraka C.E., Diver R.B., Rawlinson K.S. (2003) "Improved Alignment Technique for Dish Concentrators”, SAND2003-0258C, *Proceedings of ISEC 2003*: 2003 International Solar Energy Conference, ASME, Kohala Coast, Hawaii Island, Hawaii USA.

[5] Steffen, B.J., Andraka, C.E., Diver, R.B. (2003), "Development and Characterization of a new 2-f Alignment Method for the Advanced Dish Development System", *Proceedings of ISEC 2003*: 2003 International Solar Energy Conference, ASME, Kohala Coast, Hawaii Island, Hawaii USA.

[6] Andraka, C.E., Sadlon, S., Myer, B, Trapeznikov, K., Liebner, C. (2009), "Rapid Reflective Facet Characterization Using Fringe Reflection Techniques", *Proceedings of Energy Sustainability 2009*, ASME, San Francisco, CA USA, July 19-23.

[7] Andraka, C.E., Sadlon, S., Myer, B, Trapeznikov, K., Liebner, C. (2009), "SOFAST: Sandia Optical Fringe Analysis Slope Tool For Mirror Characterization", *Proceedings of Solar Paces 2009*, Berlin, Germany September.

[8] Bothe, T., Li, W., von Kopylow, C., Jüptner, W., (2004),"High Resolution 3D Shape Measurement on Specular Surfaces by Fringe Reflection", *Optical Metrology in Production Engineering,* Proceedings of SPIE Vol. 5457, Bellingham, WA. USA

[9] Ulmer, S., Marz, T., Prahl, C, Reinalter, W., Belhomme, B. (2011), "Automated High Resolution Measurement of Heliostat Slope Errors", *Solar Energy*, Vol 85, p681-687.

[10] Heimsath, A., Platzer, W., Bothe, T., Wansong, L. (2008), "Characterization of Optical Components for Linear Fresnel Collectors by Fringe Reflection Method", *Proceedings of Solar Paces Conference*, Las Vegas, NV USA.

[11] Andraka, C.E., Yellowhair, J., Trapeznikov, K., Carlson, J., Myer, B., Stone, B., Hunt, K. (2010) "AIMFAST: An Alignment Tool Based On Fringe Reflection Methods Applied To Dish Concentrators", *Proceedings of Solar Paces Conference,* Perpignan, France.

[12] Bouguet, Jean-Yves, (2010), "Camera Calibration Toolbox for Matlab", http://www.vision.caltech.edu/bouguetj/calib_doc/.

[13] Yellowhair, J., Andraka, C.E., Trapeznikov, K., Hunt, K. (2010) "Alignment Strategy Development For Imperfect Facets On A Dish Concentrating System", *Proceedings of Solar Paces Conference,* Perpignan, France.

[14] Romero V. J. (1991), "CIRCE2/DEKGEN2: A Software Package for Facilitated Optical Analysis of 3-D Distributed Solar Energy Concentrators – Theory and User Manual," SAND91-2238, Sandia National Laboratories, Albuquerque, NM